Rock and Soil Mechanics

Volume 44 | Issue 2 Article 1

4-10-2023

Simplified analytical solution for horizontal seismic response of single piles to vertically incident S waves

Chang-jie ZHENG
Fujian Provincial Key Laboratory of Advanced Technology and Informatization in Civil Engineering, Fujian University of Technology, Fuzhou, Fujian 350118, China, School of Civil Engineering, Fujian University of Technology, Fuzhou, Fujian 350118, China

Yi-qin CUI
Fujian Provincial Key Laboratory of Advanced Technology and Informatization in Civil Engineering, Fujian University of Technology, Fuzhou, Fujian 350118, China, School of Civil Engineering, Fujian University of Technology, Fuzhou, Fujian 350118, China

Chen WU
Fujian Provincial Key Laboratory of Advanced Technology and Informatization in Civil Engineering, Fujian University of Technology, Fuzhou, Fujian 350118, China, School of Civil Engineering, Fujian University of Technology, Fuzhou, Fujian 350118, China

Tong LUO
Fujian Provincial Key Laboratory of Advanced Technology and Informatization in Civil Engineering, Fujian University of Technology, Fuzhou, Fujian 350118, China, School of Civil Engineering, Fujian University of Technology, Fuzhou, Fujian 350118, China

Simplified analytical solution for horizontal seismic response of single piles to vertically incident S waves

Authors

Chang-jie ZHENG, Yi-qin CUI, Chen WU, Tong LUO, and Lu-bao LUAN

Rock and Soil Mechanics 2023 44(2): 327−336 ISSN 1000−7598
https: //doi.org/10.16285/j.rsm.2022.5403 http://rocksoilmech.researchcommons.org/journal

Simplified analytical solution for horizontal seismic response of single piles to vertically incident S waves

ZHENG Chang-jie[1, 2], CUI Yi-qin[1, 2], WU Chen[1, 2], LUO Tong[1, 2], LUAN Lu-bao[3]

1. Fujian Provincial Key Laboratory of Advanced Technology and Informatization in Civil Engineering, Fujian University of Technology, Fuzhou, Fujian 350118, China
2. School of Civil Engineering, Fujian University of Technology, Fuzhou, Fujian 350118, China
3. College of Environmental Science and Technology, Ocean University of China, Qingdao, Shandong 266100, China

Abstract: Based on the continuous medium model and the pile-soil interaction, the horizontal seismic response of a single pile subjected to vertically propagating S waves was investigated by regarding the single pile as a one-dimensional linearly elastic beam. The time-harmonic displacement of bedrock was introduced as the vertically propagating S waves, and the horizontal dynamic impedance function of the soil was derived by the governing equations of the plane strain model. Analytical solutions for the seismic response of the single pile subjected to vertically propagating S waves were obtained by subsuming soil impedance into the governing equation of the single pile and considering the boundary conditions at pile top and toe. The solution was verified by comparing it to the results of existing studies. Furthermore, as pile-soil modulus ratio increases, the minimum value of the kinematic response factor decreases. The kinematic response factor is not particularly sensitive to the large pile slenderness ratio and the soil material damping. For the horizontal amplification factor at the pile top, the increase of the pile-soil modulus ratio only suppresses the amplification at high resonance frequency, and the large pile slenderness ratio has the trivial effect on it. As the soil material damping increases, the amplification at resonance frequency gets considerably suppressed. The seismic response of the pile is obviously affected by the pile-soil modulus ratio only when the pile slenderness ratio is small, and it decreases with the increase of the pile-soil modulus ratio.
Keywords: S waves; pile foundation; seismic response; analytical solution

1 Introduction

Pile foundations are extensively employed in various engineering projects because of their high bearing capacity, high stability, small settlement, and good flexibility to varying geological and load conditions. In current seismic designs of buildings, the motion form of building foundations is considered to be consistent with that of the surrounding free field during earthquakes, which is conservative under certain static situations. However, oceans of engineering practices and studies[1−4] demonstrate that the displacements of the pile foundation and the surrounding soil are inconsistent during earthquakes. During an earthquake, the pile foundation vibrates due to the soil layer movement, while the soil movement is conversely affected by the pile vibration. This dynamic response of the pile under the earthquake is called the kinematic pile–soil interaction, and it has a substantial impact on the seismic analysis and design of the pile foundation and superstructure. The dynamic response of the pile is crucial to the dynamic response of the foundation–superstructure system under the earthquake excitation, and its precision directly influences the seismic design accuracy of the superstructure. Therefore, the pile–soil interaction should be fully considered while investigating the seismic capacity of the superstructure.

Once an earthquake is caused, the vibration generated from the dislocation and fracture of underground rock masses propagates outward from the focus as seismic waves, and the energy carried by the seismic waves is dominantly transmitted in the form of elastic waves. The elastic wave travelling underground is predominantly a transverse wave (shear wave or S wave), while the elastic wave travelling along the ground surface is primarily a Rayleigh wave. The elastic waves propagate from the soil to the pile foundation, and then from the pile foundation to the superstructure, causing the vibration of the superstructure. The existing research on the seismic response of pile foundations focuses on the kinematic pile–soil interaction under S waves, which has been completed using numerical simulations, model tests, and analytical approaches. The used numerical approaches consist of the finite element method[5−9] and the boundary element method[10−11]. Shen et al.[12] analyzed the seismic response of an ultra-deep pile foundation by the three-dimensional finite element method. Li et al.[13] investigated the influence of soil nonlinearity on the horizontal seismic response of a single pile using a finite element model of the single pile–foundation soil system. Kaynia[14] compared the dynamic responses of the pile foundation to different incident waves based on the boundary element method. Sen et al.[15], Senm et al.[16], and Davies et al.[17] adopted the boundary element method to examine the vertical and horizontal vibrations of the

Received: 30 March 2022 Accepted: 20 June 2022
This work was supported by the Open Fund of Key Laboratory of New Technology for Construction of Cities in Mountain Area of Ministry of Education (LNTCCMA-20220108), the National Natural Science Foundation of China (52178318), the Natural Science Foundation of Fujian Province (2021J011056), and the Young Elite Scientists Sponsorship Program by CAST (2021QNRC001).
First author: ZHENG Chang-jie, male, born in 1989, PhD, Professor, research interests: pile foundation dynamics and geotechnical seismic engineering. E-mail: zcj@fjut.edu.cn
Corresponding author: LUAN Lu-bao, male, born in 1989, PhD, Postdoctor, research interests: pile foundation dynamics. E-mail: luanlub@163.com

single pile and pile group. Chen et al.[18] explored the horizontal seismic response of pile group foundations using a simplified boundary element model of kinematic pile–soil interactions. In addition, Feng et al.[19] studied the horizontal bearing capacity of a high pile group foundation in soft soil through the physical model test and three-dimensional finite element method. Wu et al.[20] investigated the seismic response of piles in coral sand through a shaking table test. Although the finite element method and the boundary element method can solve the problems involving complex structures and soil layering, their boundary treatments are inconvenient, their computation resource consumptions are always enormous, and seismic resistance mechanisms of the pile foundation are only partially illustrated by them. Most of the available analytical approaches are based on the dynamic Winkler (BDWF) model assumption[21–24] and utilize a series of Winkler springs and damping to simulate the effects of soil surrounding the pile.

Based on the continuum theory and the plane strain model, an analytical expression for the complex dynamic impedance of the soil was deduced through the established soil model and was then substituted into the motion equation of the single pile to obtain the analytical solution for the horizontal seismic response of the single pile subjected to vertically incident S waves. The analytical solution was confirmed by comparing it to existing theoretical and finite element findings. Furthermore, the influence of the principal pile–soil system parameters on the horizontal seismic response of the single pile was quantified.

2 Definite solution problem

In the calculation sketch presented in Fig. 1, a single pile with a length of H and a diameter of D is buried in the homogeneous viscoelastic soil layer sitting on the rigid bedrock. A simple harmonic horizontal vibration $u_g e^{i\omega t}$ is applied to the bedrock to model vertically incident S waves, where u_g is the horizontal vibration amplitude of the bedrock under the earthquake, ω is the frequency of the seismic wave, and t is the time. Based on Novak's plane strain assumption, the soil is treated as an independent infinite thin layer, disregarding the vertical normal stress gradient and assuming perfect contact between the pile and the soil[6, 25]. In Fig. 1, λ and G are the Lame constants of the elastic medium, β is the hysteretic damping of the soil, ρ_s is the soil density, and v_s is Poisson's ratio of the soil. For simplicity, the time component $e^{i\omega t}$ is omitted in the following derivation.

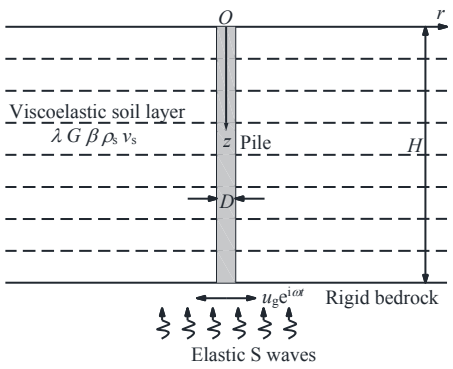

Fig. 1 Conceptual model of pile–soil system

2.1 Solution for dynamic impedance function of soil

The cylindrical coordinate system attached to the pile is shown in Fig. 2.

Fig. 2 Cylindrical coordinate system of pile

According to the elastodynamics theory, the simplified motion equation for the soil is established:

$$G^*\nabla^2 u_r + (\lambda^* + G^*)\frac{\partial e}{\partial r} - \frac{G^*}{r^2}\left(2\frac{\partial u_\theta}{\partial \theta} + u_r\right) = -\rho_s \omega^2 u_r \tag{1}$$

$$G^*\nabla^2 u_\theta + (\lambda^* + G^*)\frac{\partial e}{r\partial \theta} - \frac{G^*}{r^2}\left(u_\theta - 2\frac{\partial u_r}{\partial \theta}\right) = -\rho_s \omega^2 u_\theta \tag{2}$$

where λ^* and G^* are the complex Lame constants of the soil, $\lambda^* = \lambda(1+2i\beta)$, $G^* = G(1+2i\beta)$; u_r and u_θ are the radial and tangential displacements of the soil; the volume strain is $e = \frac{\partial u_r}{\partial r} + \frac{u_r}{r} + \frac{\partial u_\theta}{r\partial \theta}$; and $\nabla^2 = \frac{\partial^2}{\partial r^2} + \frac{1}{r}\frac{\partial}{\partial r} + \frac{1}{r^2}\frac{\partial^2}{\partial \theta^2}$.

The absolute displacement of the soil subjected to the seismic waves is expressed as the superposition of the free field displacement and the soil displacement relative to the free field displacement:

$$u_r = u_r^r + u_{ff}\cos\theta \tag{3}$$

$$u_\theta = u_\theta^r - u_{ff}\sin\theta \tag{4}$$

where u_r^r and u_θ^r are the radial and tangential soil displacements relative to the free field soil displacement under seismic waves; $u_{ff} = u_g \frac{\cos(\chi z)}{\cos(\chi H)}$ is the free field displacement[22]; and $\chi = \sqrt{\rho_s \omega^2 / G^*}$.

Equations (3) and (4) are substituted into Eqs. (1) and (2), and the differential transformation $\frac{\partial(1)}{\partial r} +$

$\frac{(1)}{r}+\frac{\partial(2)}{r\partial\theta}$ is performed to produce

$$(\lambda^*+2G^*)\nabla^2 e^{\mathrm{r}}+\rho_{\mathrm{s}}\omega^2 e^{\mathrm{r}}=0 \tag{5}$$

where $e^{\mathrm{r}}=\frac{\partial u_r^{\mathrm{r}}}{\partial r}+\frac{u_r^{\mathrm{r}}}{r}+\frac{\partial u_\theta^{\mathrm{r}}}{r\partial\theta}=e$.

$e^{\mathrm{r}}=R(r)\Phi(\theta)$ is substituted into Eq. (5) to get

$$(\lambda^*+2G^*)\left[\frac{R''(r)}{R(r)}+\frac{R'(r)}{rR(r)}+\frac{\Phi''(\theta)}{r^2\Phi(\theta)}\right]+\rho_{\mathrm{s}}\omega^2=0 \tag{6}$$

Equation (6) can be decomposed into the following ordinary differential equations:

$$\frac{R''(r)}{R(r)}+\frac{R'(r)}{rR(r)}-\frac{m^2}{r^2}=q_1^2 \tag{7}$$

$$\frac{\Phi''(\theta)}{\Phi(\theta)}=-m^2 \tag{8}$$

where $q_1^2=-\frac{\rho_{\mathrm{s}}\omega^2}{\lambda^*+2G^*}$.

The general solutions for Eqs. (7) and (8) are as follows:

$$R(r)=A_1K_m(q_1r)+B_1I_m(q_1r) \tag{9}$$

$$\Phi(\theta)=C_1\sin(m\theta)+D_1\cos(m\theta) \tag{10}$$

where $I_m(\ )$ and $K_m(\ )$ are Bessel functions of the first and the second types of order m; and A_1, B_1, C_1, and D_1 are undetermined coefficients.

The boundary condition of the soil at radial infinity[26] is

$$u_r^{\mathrm{r}}\big|_{r\to\infty}=u_\theta^{\mathrm{r}}\big|_{r\to\infty}=0 \tag{11}$$

When the Bessel function of the first type is utilized, $B_1=0$ is obtained.

The boundary condition at the pile–soil interface is

$$u_r\big|_{r=r_0}=u_{\mathrm{p}}\cos\theta,\ u_\theta\big|_{r=r_0}=-u_{\mathrm{p}}\sin\theta \tag{12}$$

where the pile radius is $r_0=D/2$; and u_{p} is the horizontal displacement of the pile under the earthquake.

When the volumetric strain e is considered as the even function of θ[27–28], $C_1=0$ and $m=1$ are obtained, and the following result is derived:

$$e^{\mathrm{r}}=A_1K_1(q_1r)\cos\theta \tag{13}$$

For simplicity, u_r^{r} and u_θ^{r} can be expressed in the following forms[29–30]:

$$\left.\begin{aligned}u_r^{\mathrm{r}}(r,\theta)&=\overline{u}_r^{\mathrm{r}}(r)\cos\theta\\ u_\theta^{\mathrm{r}}(r,\theta)&=\overline{u}_\theta^{\mathrm{r}}(r)\sin\theta\end{aligned}\right\} \tag{14}$$

Equations (13) and (14) are substituted into Eqs. (1) and (2), and the addition and subtraction of the resultant equations are conducted to return

$$G^*\left(\frac{\partial^2}{\partial r^2}+\frac{\partial}{r\partial r}-\frac{4}{r^2}\right)U+\rho_{\mathrm{s}}\omega^2U=(\lambda^*+G^*)A_1q_1K_2(q_1r) \tag{15}$$

$$G^*\left(\frac{\partial^2}{\partial r^2}+\frac{\partial}{r\partial r}\right)V+\rho_{\mathrm{s}}\omega^2V=(\lambda^*+G^*)A_1q_1K_0(q_1r) \tag{16}$$

where $U=\overline{u}_r^{\mathrm{r}}+\overline{u}_\theta^{\mathrm{r}}$ and $V=\overline{u}_r^{\mathrm{r}}-\overline{u}_\theta^{\mathrm{r}}$.

The solutions for Eqs. (15) and (16) are easily determined using the variable separation method:

$$U=\gamma A_1K_2(q_1r)+A_2K_2(q_2r) \tag{17}$$

$$V=\gamma A_1K_0(q_1r)+A_3K_0(q_2r) \tag{18}$$

where $q_2^2=-\frac{\rho_{\mathrm{s}}\omega^2}{G^*}$; $\gamma=\frac{(\lambda^*+G^*)q_1}{G^*q_1^2+\rho_{\mathrm{s}}\omega^2}$; and A_2 and A_3 are undetermined coefficients. According to the definition of volume strain, the following result is got:

$$A_3=-A_2 \tag{19}$$

As a result, u_r and u_θ can be stated as

$$u_r=\left[\gamma A_1\frac{K_2(q_1r)+K_0(q_1r)}{2}+A_2\frac{K_2(q_2r)-K_0(q_2r)}{2}\right]\cdot\cos\theta+u_{\mathrm{ff}}\cos\theta \tag{20}$$

$$u_\theta=\left[\gamma A_1\frac{K_2(q_1r)-K_0(q_1r)}{2}+A_2\frac{K_2(q_2r)+K_0(q_2r)}{2}\right]\cdot\sin\theta-u_{\mathrm{ff}}\sin\theta \tag{21}$$

According to the continuity conditions at the pile–soil interface, the following result is obtained:

$$A_2=\delta A_1 \tag{22}$$

where $\delta=-\frac{\gamma K_2(q_1r_0)}{K_2(q_2r_0)}$.

According to the stress–strain relationship, the normal stress σ_r of the soil is

$$\sigma_r=(\lambda^*+2G^*)\frac{\partial u_r}{\partial r}+\lambda^*\frac{u_r}{r}+\lambda^*\frac{\partial u_\theta}{r\partial\theta} \tag{23}$$

The shear stress $\tau_{r\theta}$ is

$$\tau_{r\theta}=\frac{G^*}{r}\frac{\partial u_r}{\partial\theta}+G^*\frac{\partial u_\theta}{\partial r}-G^*\frac{u_\theta}{r} \tag{24}$$

Substituting Eqs. (20) and (21) into Eqs. (23) and (24) leads to

$$\sigma_r=A_1\left[(\lambda^*+2G^*)K_1(q_1r)-2G^*\gamma\frac{K_2(q_1r)}{r}-2G^*\delta\frac{K_2(q_2r)}{r}\right]\cos\theta \tag{25}$$

$$\tau_{r\theta}=-G^{*}A_1\left[2\gamma\frac{K_2(q_1r)}{r}+2\delta\frac{K_2(q_2r)}{r}+\delta q_2K_1(q_2r)\right]\sin\theta \tag{26}$$

The horizontal resistance f of the soil to the pile[26] can be written as

$$f=-\int_0^{2\pi}(\sigma_r\cos\theta-\tau_{r\theta}\sin\theta)\big|_{r=r_0}r_0\mathrm{d}\theta=-\pi r_0A_1\left[(\lambda^{*}+2G^{*})K_1(q_1r_0)+\delta G^{*}q_2K_1(q_2r_0)\right] \tag{27}$$

The horizontal complex dynamic impedance K of the soil along the pile can then be calculated as

$$K=\frac{f}{u_r\big|_{r=r_0,\theta=0}-u_{\mathrm{ff}}}=\frac{-\pi D\left[(\lambda^{*}+2G^{*})K_1(q_1r_0)+\delta G^{*}q_2K_1(q_2r_0)\right]}{\gamma\left[K_2(q_1r_0)+K_0(q_1r_0)\right]+\delta\left[K_2(q_2r_0)-K_0(q_2r_0)\right]} \tag{28}$$

2.2 Solution for governing equations of pile

Considering the stress balance of the pile, the dynamic governing equation of the pile is

$$E_{\mathrm{p}}I_{\mathrm{p}}\frac{\partial^4u_{\mathrm{p}}}{\partial z^4}-\rho_{\mathrm{p}}A_{\mathrm{p}}\omega^2u_{\mathrm{p}}+K(u_{\mathrm{p}}-u_{\mathrm{ff}})=0 \tag{29}$$

where E_{p} is the elastic modulus of the pile; I_{p} is the inertia moment of the pile section; ρ_{p} is the density of the pile; and A_{p} is the area of the pile section.

Both sides of Eq. (29) are adjusted to obtain

$$\frac{\mathrm{d}^4u_{\mathrm{p}}}{\mathrm{d}z^4}-\kappa^4u_{\mathrm{p}}=\frac{K}{E_{\mathrm{p}}I_{\mathrm{p}}}u_{\mathrm{ff}} \tag{30}$$

where $\kappa=\left(\dfrac{\rho_{\mathrm{p}}A_{\mathrm{p}}\omega^2-K}{E_{\mathrm{p}}I_{\mathrm{p}}}\right)^{1/4}$.

The solution for Eq. (30) is

$$u_{\mathrm{p}}=N_1\sin(\kappa z)+N_2\cos(\kappa z)+N_3\sinh(\kappa z)+N_4\cosh(\kappa z)+\zeta u_{\mathrm{ff}} \tag{31}$$

where N_1-N_4 are undetermined coefficients and $\zeta=\dfrac{K}{E_{\mathrm{p}}I_{\mathrm{p}}(q_2^4-\kappa^4)}$.

The rotation angle ϕ_{p}, bending moment M_{p}, and shear force Q_{p} of the pile can be written as

$$\phi_{\mathrm{p}}=\kappa N_1\cos(\kappa z)-\kappa N_2\sin(\kappa z)+\kappa N_3\cosh(\kappa z)+\kappa N_4\sinh(\kappa z)+\zeta u_{\mathrm{g}}\frac{q_2\sinh(q_2z)}{\cosh(q_2H)} \tag{32}$$

$$\frac{M_{\mathrm{p}}}{E_{\mathrm{p}}I_{\mathrm{p}}}=-\kappa^2N_1\sin(\kappa z)-\kappa^2N_2\cos(\kappa z)+\kappa^2N_3\cdot\sinh(\kappa z)+\kappa^2N_4\cosh(\kappa z)+\zeta u_{\mathrm{g}}\frac{q_2^2\cosh(q_2z)}{\cosh(q_2H)} \tag{33}$$

$$\frac{Q_{\mathrm{p}}}{E_{\mathrm{p}}I_{\mathrm{p}}}=-\kappa^3N_1\cos(\kappa z)+\kappa^3N_2\sin(\kappa z)+\kappa^3N_3\cdot\cosh(\kappa z)+\kappa^3N_4\sinh(\kappa z)+\zeta u_{\mathrm{g}}\frac{q_2^3\sinh(q_2z)}{\cosh(q_2H)} \tag{34}$$

The solutions for the pile response under arbitrary boundary conditions can be collected from Eqs. (31) to (34). The following typical boundary conditions at the pile top and bottom are considered[22]:

Free pile top:

$$M_{\mathrm{p}}\big|_{z=0}=0,\quad Q_{\mathrm{p}}\big|_{z=0}=0 \tag{35}$$

Fixed pile top:

$$\phi_{\mathrm{p}}\big|_{z=0}=0,\quad Q_{\mathrm{p}}\big|_{z=0}=0 \tag{36}$$

Free pile bottom:

$$M_{\mathrm{p}}\big|_{z=H}=0,\quad Q_{\mathrm{p}}\big|_{z=H}=0 \tag{37}$$

Fixed pile bottom:

$$u_{\mathrm{p}}\big|_{z=H}=u_{\mathrm{g}},\quad \phi_{\mathrm{p}}\big|_{z=H}=0 \tag{38}$$

Equations (31) to (34) are substituted into the above different boundary conditions at the pile top and bottom, yielding a system of linear equations with 4 variables. The displacement and stress of the pile can be given by solving the system of linear equations.

The kinematic pile–soil response factor I_{u} [6] is defined as

$$I_{\mathrm{u}}=\left|\frac{u_{\mathrm{p}}(0)}{u_{\mathrm{ff}}(0)}\right| \tag{39}$$

3 Verification and parameter analysis

The derived analytical solutions are attained by programming in Mathematica or Matlab software, and the horizontal seismic response of the single pile under any boundary condition at the pile top and bottom can be calculated quickly. First, the results calculated using the derived solution are verified in comparison with the calculation results based on the Winkler foundation model of Anoyatis et al.[22], the modified Vlasov model of Liu et al.[25], and the finite element results of Gazetas[5]. Then, the effects of the pile–soil modulus ratio, pile slenderness ratio, and soil damping on the kinematic pile–soil response factor, horizontal amplification factor at the pile top, and pile displacement and strain are explored based on the derived analytical solutions, and the variation law of the horizontal dynamic impedance of the soil is examined. Unless particular descriptions are presented, the boundary conditions of free pile top and fixed pile bottom are employed in the following analysis. The calculation parameters are: $H/D=20$, $v_{\mathrm{s}}=0.4$, $\beta=0.05$, and $\rho_{\mathrm{s}}/\rho_{\mathrm{p}}=0.7$, where E_{s} is the elastic modulus of the soil. The dimensionless frequency $a_0=\omega D/V_{\mathrm{s}}$ is used in the calculation, where $V_{\mathrm{s}}=\sqrt{G/\rho_{\mathrm{s}}}$ is the S wave velocity of the soil.

Figures 3 and 4 display the kinematic response factor calculated with the present solution compared to

the analytical findings of Anoyatis et al.[22] and Liu et al.[25] and the FEM results of Gazetas[5]. For the results displayed in Fig. 3, the boundary conditions of free pile top and bottom are specified in the present solution, which is consistent with those of Anoyatis et al.[22] and Liu et al.[25]. For the results displayed in Fig. 4, the boundary conditions of fixed pile bottom and free pile top are determined in the present solution, which is consistent with those of Gazetas[5], and the pile and soil parameters highlighted in the figure are picked from the model C (homogeneous soil) of Gazetas[5], where f_1 is the first resonance frequency of the soil layer. As shown in Figs. 3 and 4, the present solution agrees well with the existing results, which verifies the correctness of the present solution.

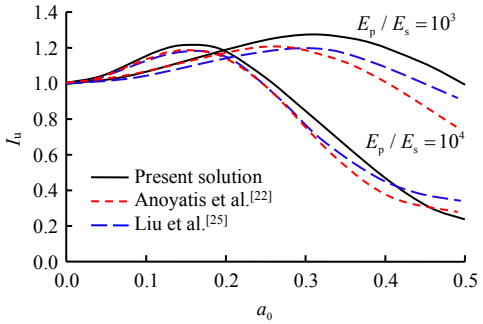

Fig. 3 Comparison of kinematic response factor calculated with present solution against results of Anoyatis et al.[22] and Liu et al.[25]

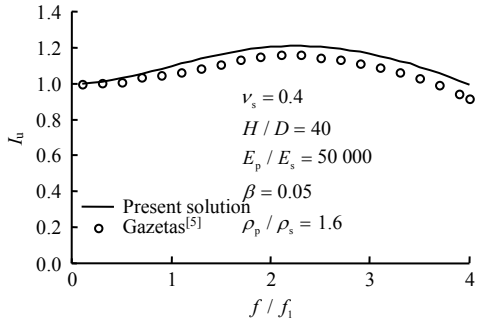

Fig. 4 Comparison of kinematic response factor calculated with present solution against FEM results of Gazetas[5]

3.1 Kinematic pile–soil response factor

The existing findings[6, 31] indicate that there are two critical frequencies a_{01} and a_{02} for the kinematic pile–soil response factor. The curves of kinematic response factor I_u with frequency are separated into three distinct regions, as depicted in Fig. 5.

(1) Within the low-frequency region ($0 < a_0 < a_{01}$), $I_u \approx 1$ implies that the pile and soil deformations are identical, and the kinematic pile–soil interaction can be neglected. In this region, the existence of the pile is irrelevant to the seismic response of the superstructure in the pile–soil system.

(2) Within the medium frequency region ($a_{01} < a_0 < a_{02}$), I_u declines rapidly with the increase of the frequency, indicating that the incompatibility and kinematic interaction between the pile and the soil rise progressively. Due to the presence of the pile, the seismic wave energy reaching the superstructure in the pile–soil system is weakened.

(3) Within the relatively high-frequency region ($a_0 > a_{02}$), I_u fluctuates in a low-value range of about 0.2–0.4, indicating the strongest kinematic pile–soil interaction occurs, and the seismic wave energy reaching the superstructure in the pile–soil system is greatly reduced due to the existence of the pile.

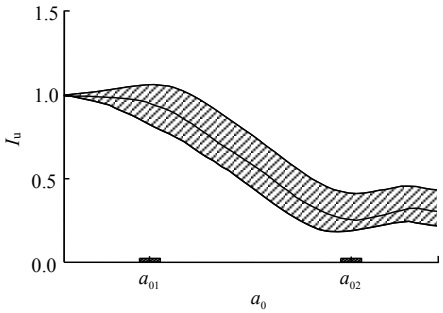

Fig. 5 Curves of kinematic response factor versus dimensionless frequency[6]

Figure 6 presents the variations of the kinematic pile–soil response factor with the dimensionless frequency under four different boundary conditions at the pile top and bottom described in Eqs. (35) to (38). As shown in Fig. 6, the boundary condition at the pile bottom has little influence on the kinematic pile–soil response factor, while the boundary condition at the pile top has a significant influence. The two critical frequencies a_{01} and a_{02} under the fixed pile top condition are significantly less than those under the free pile top condition, and the kinematic pile–soil response factor under the fixed pile top condition is significantly less than that under the free pile top condition, indicating that the seismic wave energy transmitted to the upper part of the pile with fixed pile top is significantly less than that with free pile top.

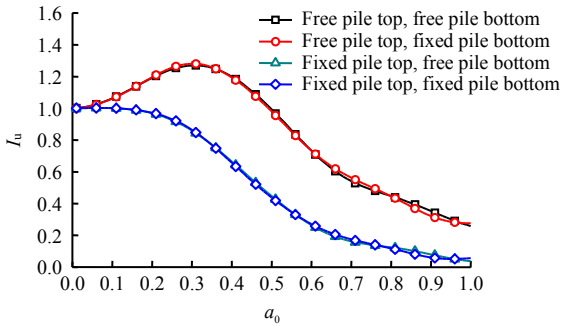

Fig. 6 Variation of kinematic response factor with dimensionless frequency under different boundary conditions at pile top and toe

The variations of the kinematic pile–soil response factor calculated using the derived solution with the modulus ratio E_p / E_s for different pile slenderness ratios are shown in Fig. 7. When $H / D = 5$ the first

critical frequency a_{01} is in a very low-frequency range for any E_p / E_s, as shown in Fig. 7 (a). When E_p / E_s is as low as 1 000, the kinematic pile–soil response factor remains over 0.9, indicating that the seismic wave energy reaching the pile top cannot be filtered for piles with low modulus when $0 < a_0 < 0.5$. As E_p / E_s increases to a higher value, the second critical frequency a_{02} decreases and the minimum I_u gradually decreases to about 0.2 due to the enhanced kinematic pile–soil interaction. In the frequency region $a_0 > a_{02}$, I_u shows a rising trend, indicating that strong high-frequency ground motions cannot be effectively mitigated when $H / D = 5$. When $H / D = 40$, the first critical frequency a_{01} is more than 0.1 because the kinematic pile–soil interaction cannot play an effective role at low frequencies when the pile flexibility is greater, as shown in Fig. 7 (b). With the increase of E_p / E_s, the first critical frequency a_{01} decreases, and the lowest I_u and the second critical frequency a_{02} decrease, indicating that the high-frequency ground motion reaching the pile top can be effectively filtered when $H / D = 40$.

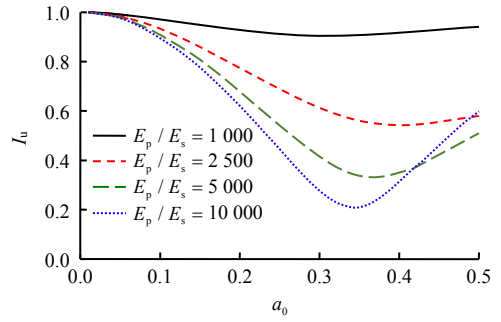

(a) $H / D = 5$

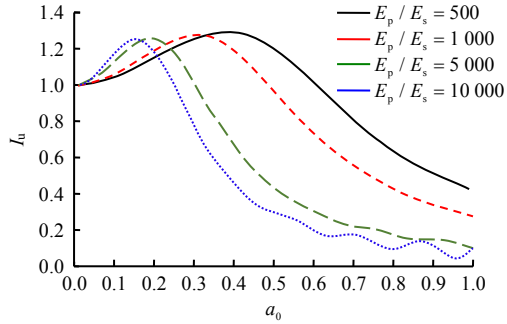

(b) $H / D = 40$

Fig. 7 Influence of pile–soil modulus ratio E_p / E_s on kinematic response factor

Figure 8 displays the variations of the kinematic pile–soil response factor in the frequency domain calculated using the derived solution for different slenderness ratios when $E_p / E_s = 10\ 000$ and $E_p / E_s = 1\ 000$. When $E_p / E_s = 10\ 000$, the two critical frequencies a_{01} and a_{02} increase with the increasing pile slenderness ratio H / D. When H / D reaches a higher value (H / D= 20), the variation of I_u with H / D can be ignored. When $E_p / E_s = 1\ 000$, H / D has little effect on the I_u curves except for $H / D = 5$.

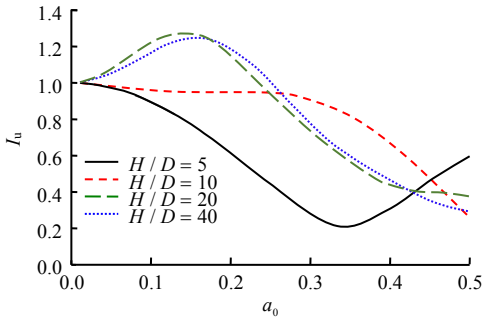

(a) E_p / E_s = 10 000

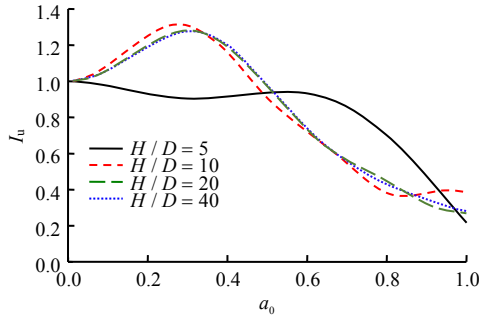

(b) E_p / E_s = 1 000

Fig. 8 Influence of pile slenderness ratio on kinematic response factor

The variations of I_u with the dimensionless frequency for three different soil damping β when $E_p / E_s = 10\ 000$ and $E_p / E_s = 1\ 000$ are given in Fig. 9. As indicated in Fig. 9, the influence of the soil damping β on the first and second critical frequencies is not significant under varied pile–soil modulus ratios.

3.2 Horizontal seismic amplification factor at pile top

In addition to the kinematic pile–soil response factor I_u, the horizontal seismic amplification factor at the pile top A_u, or the ratio of the horizontal displacement at the pile top to the bedrock displacement, is introduced:

$$A_u = \left| \frac{u_p(0)}{u_g} \right| \tag{40}$$

The variations of the horizontal seismic amplification factor at the pile top with the dimensionless frequency for different E_p / E_s and H / D are depicted in Figs. 10 and 11. As seen in Fig. 10, there are resonance frequencies for the curves of the horizontal seismic amplification factor at the pile top, and the horizontal seismic amplification factor at the pile top reaches its maximum at the first resonance frequency. These resonance frequencies in Fig. 10 correspond to the natural frequency of the soil layer[25]:

$$\omega_n = \frac{V_s(2n-1)\pi}{2H} \tag{41}$$

where n is the positive integer.

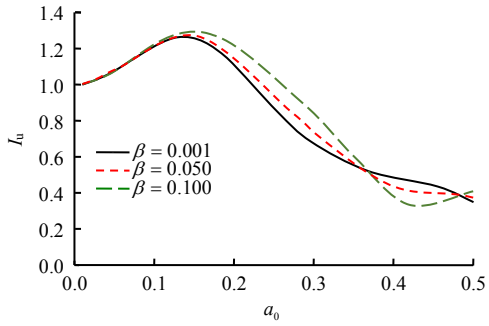

(a) $E_p / E_s = 10\,000$

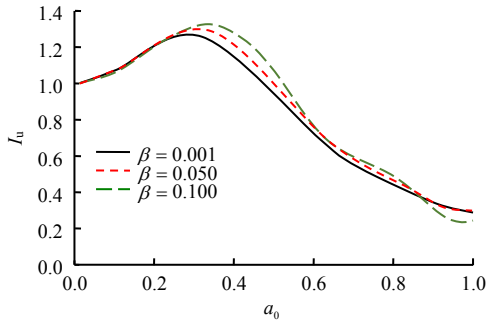

(b) $E_p / E_s = 1\,000$

Fig. 9 Influence of soil damping on kinematic response factor

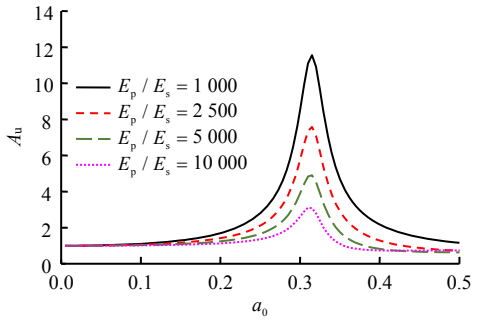

(a) $H / D = 5$

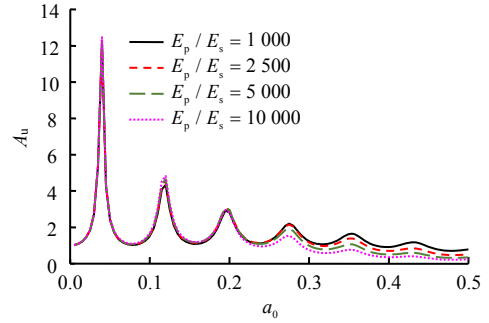

(b) $H / D = 40$

Fig. 10 Influence of pile–soil modulus ratio E_p / E_s on horizontal amplification factor at pile top

As illustrated in Fig. 10, the horizontal seismic amplification factor at the pile top corresponding to the resonance frequency decreases with the increasing pile–soil modulus ratio E_p / E_s when $H / D = 5$. When $H / D = 40$, the increase of E_p / E_s has little effect on the amplification factor at the first several resonant frequencies, while the increase of E_p / E_s at the high frequency causes the decrease of the horizontal seismic amplification factor at the pile top corresponding to the resonance frequencies. As illustrated in Fig. 11, H / D mainly affects the resonance frequency. As demonstrated in Eq. (41), the resonance frequency is closely related to the pile length. Except for $H / D = 5$, the influence of H / D on the resonance amplitude of the horizontal seismic amplification factor at the pile top is not obvious.

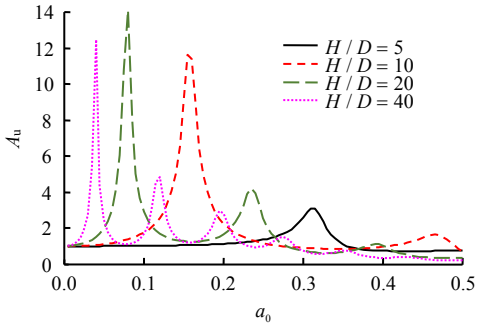

(a) $E_p / E_s = 10\,000$

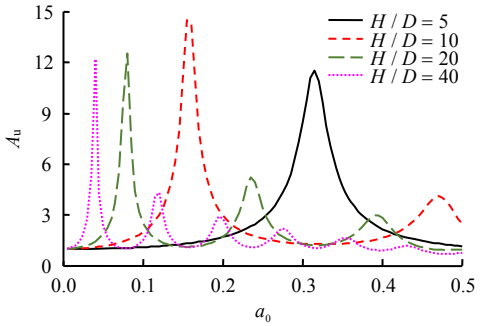

(b) $E_p / E_s = 1\,000$

Fig. 11 Influence of pile slenderness ratio *H/D* on horizontal amplification factor at pile top

The effect of the soil damping on the horizontal seismic amplification factor at the pile top is displayed in Fig. 12. As the soil damping rises, more seismic vibration energy is absorbed by the soil, and the horizontal seismic amplification factor at the pile top corresponding to the resonance frequency is greatly suppressed.

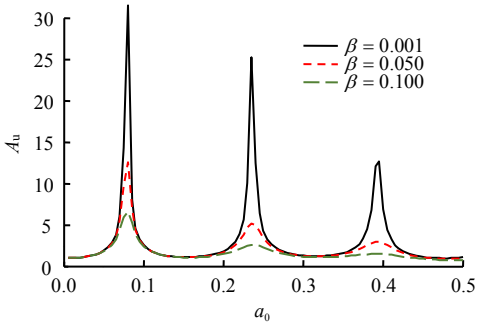

Fig. 12 Influence of soil damping on horizontal amplification factor at pile top

3.3 Pile displacement and strain

Figures 13 and 14 describe the influence of the pile–soil modulus ratio E_p / E_s at the resonance frequency of the first soil layer ω_1 ($\omega_1 = V_s \pi / 2H$) on the horizontal displacement, rotation angle, bending strain, and shear strain of the pile when H/D=5 and H/D=40.

When H/D=5, all dynamic responses are significantly reduced with the increase of E_p / E_s. When H/D=40, the change of E_p / E_s has little effect on the horizontal displacement of the pile, while the rotation angle, bending strain, and shear strain slightly decrease as E_p / E_s grows, but their effects are considerably less than those of the pile with a small slenderness ratio.

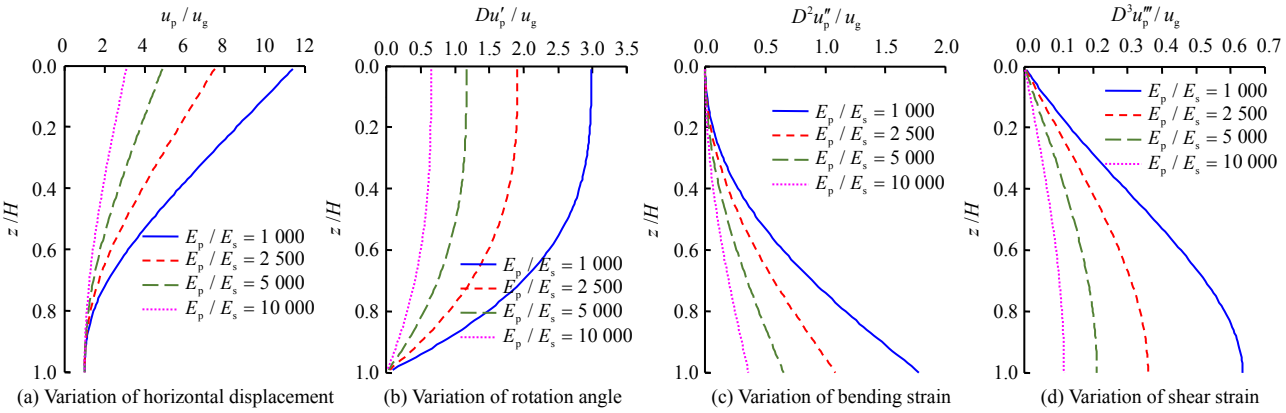

Fig. 13 Variations of horizontal displacement, rotation angle, bending strain, and shear strain with pile–soil modulus ratio E_p / E_s ($\omega = \omega_1$, H/D=5)

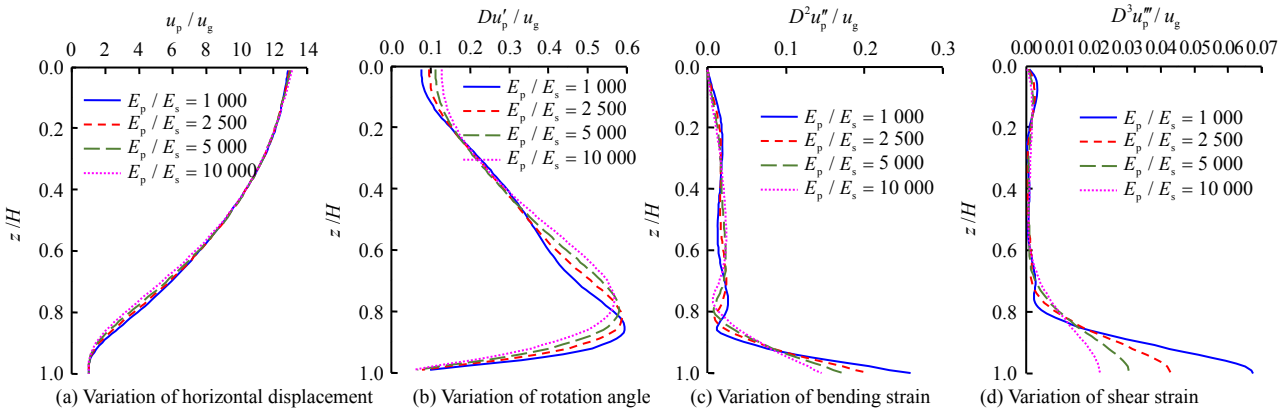

Fig. 14 Variations of horizontal displacement, rotation angle, bending strain, and shear strain with pile–soil modulus ratio E_p / E_s ($\omega = \omega_1$, H/D=40)

4 Conclusion

Based on the plane strain model, a simplified analytical solution for the horizontal seismic response of the single pile to vertically incident S waves was derived considering the pile–soil interaction. It is worth noting that the derived analytical solution is simply the elastic solution compared to the finite element findings, which cannot consider the plastic deformation of the pile and soil, as well as the complex pile section and foundation layering. The derived analytical solution has the benefits of avoiding complex modeling and lengthy computation. Based on the derived analytical solution, the horizontal seismic response of the single pile in homogeneous soil was investigated, and the following conclusions are obtained:

(1) When the pile slenderness ratio is low, the kinematic pile–soil interaction begins at a very low frequency, but the kinematic pile–soil response factor always keeps high. When the pile–soil modulus is relatively small, the second critical frequency is quite high, and it decreases with increasing the relative stiffness of the pile. However, within the frequency range greater than the second critical frequency, I_u increases and reaches a larger value, indicating that the high-frequency vibration cannot be effectively mitigated for small pile slenderness ratios. When the pile slenderness ratio is large, the first critical frequency is higher, and the first and second critical frequencies and the kinematic pile–soil response factor decrease as the relative rigidity of the pile increases, indicating that the high-frequency vibration reaching the pile top can be effectively filtered out by increasing the slenderness ratio.

(2) When the pile–soil modulus ratio is relatively large, the first and second critical frequencies of the kinematic pile–soil response factor rise as the slender-

ness ratio increases. When the slenderness ratio reaches a critical threshold, the kinematic pile–soil response factor curves do not change with the slenderness ratio. When the pile stiffness is small, the slenderness ratio has little effect on the kinematic pile–soil response factor except for the minimum slenderness ratio.

(3) The horizontal seismic amplification factor at the single pile top exhibits resonance phenomena at the resonance frequency of the soil layer, with the resonance effect being the most significant at the first resonance frequency. When the pile slenderness ratio is small, the horizontal seismic amplification factor at the pile top corresponding to the resonance frequency decreases with the increasing relative stiffness of the pile. However, when the pile slenderness ratio increases, the increase of the relative stiffness of the pile has little effect on the amplification factor at the first several resonance frequencies, and the increase of the relative stiffness of the pile at the high frequency reduces the horizontal seismic amplification factor at the resonance frequencies. The pile slenderness ratio mainly affects the resonance frequency, but has no obvious effect on the resonance amplitude of the horizontal seismic amplification factor at the pile top.

(4) The first critical frequency of the kinematic pile–soil response factor increases with the increase of the soil damping, whereas the resonance amplitude of the horizontal seismic amplification factor at the pile top obviously decreases.

(5) When the pile slenderness ratio is low, the horizontal displacement, rotation angle, bending strain, and shear strain of the pile decrease obviously as the relative rigidity of the pile increases. For piles with a large slenderness ratio, increasing the relative stiffness of the pile only slightly affects the displacement and strain at the pile bottom, and has little effect on the upper part of the pile.

References

[1] WANG Kai-shun. Impedance of subsoil and seismic response of structures[J]. Earthquake Engineering and Engineering Vibration, 1985, 5(2): 87–102.

[2] LI Yu-run, YUAN Xiao-ming, LIANG Yan, et al. Analysis for *p-y* curves of liquefied soil-pile interaction[J]. Earthquake Engineering and Engineering Vibration, 2008, 28(3): 165–171.

[3] LIU Lin-chao, YANG Xiao. Dynamic interaction of saturated soil-pile-structure system under seismic loading[J]. Rock and Soil Mechanics, 2012, 33(1): 120–128.

[4] DAI D H, EL NAGGAR M H, ZHANG N, et al. Kinematic response of an end-bearing pile subjected to vertical P-wave considering the three-dimensional wave scattering[J]. Computers and Geotechnics, 2020, 120: 103368.

[5] GAZETAS G. Seismic response of end-bearing single piles[J]. International Journal of Soil Dynamics and Earthquake Engineering, 1984, 3(2): 82–93.

[6] FAN K, GAZETAS G, KAYNIA A, et al. Kinematic seismic response of single piles and pile groups[J]. Journal of Geotechnical Engineering, 1991, 117(12): 1860–1879.

[7] ZHANG Su-zhen, ZHENG Qi-zhen, WANG Jing-jing, et al. Numerical analysis of dynamic response for single pile under horizontal seismic action[J]. Journal of Water Resources and Water Engineering, 2013, 24(6): 6–10.

[8] GAO Meng, XU Xiao, WANG Ying, et al. The seismic response performance of large-diameter belled pile[J]. Earthquake Engineering and Engineering Dynamics, 2018, 38(3): 194–202.

[9] WAN Jian-hong, ZHENG Xiang-zhi, OUYANG Wei-hang, et al. Stability analysis of single pile base on efficient finite-element method[J]. Rock and Soil Mechanics, 2020, 41(8): 2805–2813.

[10] PAK R Y S, JI F. Mathematical boundary integral equation analysis of an embedded shell under dynamic excitations[J]. International Journal for Numerical Methods in Engineering, 1994, 37(14): 2501–2520.

[11] SHI Gang, GAO Guang-yun. Semi-analytical boundary element method in saturated soil and its application to analysis of double row of piles as passive barriers[J]. Rock and Soil Mechanics, 2010, 31(Suppl.2): 59–64.

[12] SHEN Ting, LI Guo-ying, ZHANG Wei-min. Effective stress finite element analysis for seismic response of deep pile foundation[J]. Rock and Soil Mechanics, 2004, 25(7): 1045–1049.

[13] LI Ya-dan, LIU Zhong, DENG Feng-qiao, et al. 3D FEM numerical simulation of single pile's lateral nonlinear dynamic rsponse under horizontal seismic[J]. Highway Engineering, 2007, 32(4): 33–36.

[14] KAYNIA A M. Dynamic stiffness and seismic response of pile groups[D]. Cambridge: Massachusetts Institute of Technology, 1982.

[15] SEN R, DAVIES T G, BANERJEE P K. Dynamic analysis of piles and pile groups embedded in homogeneous soils[J]. Earthquake Engineering and Structural Dynamics, 2010, 13(1): 53–65.

[16] SENM R, KAUSEL E, BANERJEE P K. Dynamic analysis of piles and pile groups embedded in non-homogeneous soils[J]. International Journal for Numerical and Analytical Methods in Geomechanics, 1985, 9(6): 507–524.

[17] DAVIES T G, SEN R, BANERJEE P K. Dynamic

behavior of pile groups in inhomogeneous soil[J]. Journal of Geotechnical Engineering, 1985, 111(12): 1365–1379.

[18] CHEN Hai-bing, LIANG Fa-yun. Simplified boundary element method for lateral vibration response of pile groups in frequency domain[J]. Chinese Journal of Geotechnical Engineering, 2014, 36(6): 1057–1063.

[19] FENG Jun, ZHANG Jun-yun, ZHU Ming, et al. Characteristic study of horizontal bearing capacity and pile group effect coefficient of laterally loaded high pile group foundation for bridge in soft soil[J]. Rock and Soil Mechanics, 2016, 37(Suppl.2): 94–104.

[20] WU Qi, DING Xuan-ming, CHEN Zhi-xiong, et al. Seismic response of pile-soil-structure in coral sand under different earthquake intensities[J]. Rock and Soil Mechanics, 2020, 41(2): 571–580.

[21] HU An-feng, XIE Kang-he, YING Hong-wei, et al. Analytical theory of lateral vibration of single pile in visco-elastic subgrade considering shear deformation[J]. Chinese Journal of Rock Mechanics and Engineering, 2004, 23(9): 1515–1520.

[22] ANOYATIS G, LAORA R D, MANDOLINI A, et al. Kinematic response of single piles for different boundary conditions: analytical solutions and normalization schemes[J]. Soil Dynamics and Earthquake Engineering, 2013, 44: 183–195.

[23] KE W H, ZHANG C. A closed-form solution for kinematic bending of end-bearing piles[J]. Soil Dynamics and Earthquake Engineering, 2017, 103: 15–20.

[24] XIONG Hui, YANG Feng. Horizontal vibration response analysis of pile foundation in liquefied soil under Winkler foundation model[J]. Rock and Soil Mechanics, 2020, 41(1): 103–110.

[25] LIU Q J, DENG F J, HE Y B. Transverse seismic kinematics of single piles by a modified Vlasov model[J]. International Journal for Numerical and Analytical Methods in Geomechanics, 2014, 38(18): 1953–1968.

[26] NOGAMI T, NOVAK M. Resistance of soil to a horizontally vibrating pile[J]. Earthquake Engineering and Structural Dynamics, 1977, 5(3): 249–261.

[27] YU Jun, SHANG Shou-ping, LI Zhong, et al. Dynamical characteristics of an end bearing pile embedded in saturated soil under horizontal vibration[J]. Chinese Journal of Geotechnical Engineering, 2009, 31(3): 408–415.

[28] ZHENG Chang-jie, LIU Han-long, DING Xuan-ming, et al. Analytical solution of horizontal vibration of cast-in-place large-diameter pipe piles in saturated soils[J]. Chinese Journal of Geotechnical Engineering, 2014, 36(8): 1447–1454.

[29] ZHANG Min, WANG Xing-hua, FENG Guo-rui. Horizontal vibration of an end-bearing pile in unsaturated soil[J]. Rock and Soil Mechanics, 2015, 36(2): 409–422.

[30] JIN B, ZHOU D, ZHONG Z. Lateral dynamic compliance of pile embedded in poroelastic half space[J]. Soil Dynamics and Earthquake Engineering, 2001, 21(6): 519–525.

[31] NOVAK M. Dynamic stiffness and damping of piles[J]. Canadian Geotechnical Journal, 1974, 11(4): 574–598.